An Investigation on the Application of Different QSPR Approaches to Identify Efficient Extractants Based on Phosphoryl-Containing Podands

Maryam Salahinejad* and Ali Roozbahani

Nuclear Science and Technology Research Institue, Tehran, Iran

Three-dimensional (3D) and two-dimensional (2D) quantitative structure-property relationship (QSPR) models were established for the computer-aided design of new phosphorus-containing podands extractants of the uranyl cation. GRIND methodology, where descriptors are derived from GRID molecular interaction fields (MIF), and Dragon-generated descriptors were used to perform QSPR modeling of the distribution coefficient (logD). The best model for 3D-QSPR has been obtained with $R2 = 0.93$ and $Q2 = 0.79$. Some simple 2D-QSPR models, able to correlate and predict the logD, are developed. The final models satisfied a set of rigorous validation criteria and performed well in the prediction of an external test set. The results reveal the role of size and steric hindrance of the hydrophobic part of the extractant molecule, as well as the importance of electrostatics and charge transfer interactions in the distribution coefficient of uranyl cation. This information could be very useful to design the most efficient ligands and find new extractants for uranyl ion extraction.

INTRODUCTION

Solvent extraction methods which involve the distribution of different components between two immiscible solvents are one of the most convenient and suitable procedures for the separation of metal ions. This method is most widely used for the separation and preconcentration of elements [1]. Because of growing interest in developing efficient and selective chelating agents, this technique has become more useful in recent years to determine trace metals [2,3].

Due to the significant influence of structural aspects of the complexing extractant agents on the efficiency of solvent extraction, many investigations have been devoted to establishing methodologies for designing more efficient ligands possessing high affinity and selectivity to specified metal ions [4-6]. The design and development of new organic ligands for selective metal ions recognition, extraction, and

separation, is of great interest in several areas of separation science and technology. Molecular modeling approaches, as powerful tools, have great potential for in silico design of novel molecular ligands with specific properties in complexation processes and extraction systems of metal ions [7,6,8,9]. Quantum mechanics [10,11], force-field molecular modeling [12], dynamic simulations [13,14], and quantitative structure-property/activity relationships (QSPR/QSAR) are three theoretical approaches that can be used for computer-aided designs of new extractants [15-17].

QSPR/QSAR studies, as progressive tools in the modeling and prediction of many physiochemical properties, allow cost savings by reducing the laboratory resources needed and the time required to investigate and design new compounds by desired properties [18]. QSAR techniques aim to develop consistent relationships between any property or activity and physicochemical properties for a series of compounds so that these "rules" can be used to evaluate new chemical entities [19]. Varnek and co-workers reported several investigations on QSPR and "In Silico" design of new

---

*Corresponding author. E-mail: salahinejad@gmail.com

extractants for several extraction systems [20-23,8,9]. They also published a comprehensive chapter book on quantitative structure-property relationships in solvent extraction and complexation of metals [8] and reviewed publications on QSPR modeling of metal complexation and extraction. Recently, Changes and co-workers [24] published a comprehensive paper on the potential and limits of QSPR and molecular modeling methods for identifying new extractants.

Three-dimensional QSAR, which refers to the use of force field calculations to compute spatial properties of three-dimensional structure (3D) of compounds, provides valuable information about the forces and interactions between two molecules [25,26] and is used as a powerful procedure in the design of new compounds of the desired property. The Grid Independent (GRIND) 3D-QSAR as an alignment-independent, interpretable, and efficient procedure to compute descriptors derived from GRID molecular interaction fields, was proved relevant in diverse structure-activity relationship studies [27,16].

In previous attempts, we investigated the application of QSPR studies in the complexation of metal ions with crown ethers [28] and the separation factor of multidentate nitrogen heterocyclic ligands in the actinides/lanthanides separation process [29]. Herein, we report GRid-INdependent Descriptors (GRIND)-based 3D-QSPR and 2D-QSPR analysis to develop valid and predictive QSPR models and estimate the distribution coefficient for the complexes of uranyl cation with phosphoryl-containing podand ligands.

MATERIALS AND METHODS

Chemical structures, experimental and predicted distribution coefficients (logD) of U(VI) extracted by phosphoryl-containing podands.

The experimental data of distribution coefficients (logD) of uranyl cation extracted from 2 M HNO_3 aqueous solution in 1,2-dichloroethane by podands (0.01 M) at 291 $^\circ$K were taken from [30]. The dataset includes 40 phosphorus-containing ligands whose chemical structures and experimental logD values are shown in Table 1. We also used the compound of the "Blind Test" set of Varnek *et al.* work [23] as an external set to validate the QSPR models obtained. Table 1 displayed the chemical structure of phosphoryl-containing podand ligands along with their experimental logD values.

The three-dimensional structure of the molecules was constructed using the standard tools available in SYBYL 7.3 molecular modeling package. Energy minimization was performed using the Tripos force field with a distance-dependent dielectric and the Powell conjugate gradient algorithm with a convergence criterion of 0.001 kcal mol^{-1} Å^{-1}. Partial atomic charges were calculated using the Gasteiger-Hückel method.

GRIND was calculated automatically using the software Pentacle, version1.05 (Molecular Discovery Ltd., Oxford, UK). The Pentacle software uses alignment-independent descriptors derived from GRID molecular interaction fields (MIF). In this study, we generated MIFs for DRY, N_1, O, and TIP probes defined as follows: the DRY probe represents hydrophobic interactions, N_1 (amide) and O (carbonyl) probes represent hydrogen bond donor and acceptor groups, respectively, and the TIP probe represents a shape-field. All molecular interaction fields were computed with a grid resolution of 0.5 Å with a smoothing window of 0.8 Å. AMANDA algorithm [31] was used for the extraction of nodes from the obtained MIF, the distance and relative position of nodes were described by $MACC_2$.

The GRIND working procedure involves three steps: (a) computing a set of molecular interaction fields (MIFs), (b) filtering the MIFs to extract the most relevant regions, and (c) encoding geometrical relationships into GRIND by computing the product of the interaction energy for each pair of filtered points (nodes). When MIF is computed for the ligand molecules, the region showing favorable energies of interaction represents positions where ligand molecules would interact favorably with metal ions. Dragon software, version 6. (TALETE srl, Italy) has been used to compute molecular descriptors.

The generated descriptors were first analyzed for the existence of constant or near-constant variables and those detected were removed. In addition, to reduce redundancy in the descriptor data matrix, the correlation of the descriptors with each other and with the dependent variable (logD) was examined. Among the collinear descriptors (r > 0.9), those with the highest correlation with logD were retained and the others were removed from the data matrix. Subsequently, an enhanced replacement method (ERM) [32,33] and fractional factorial design (FFD) [34] were used to extract the more

Table 1. Chemical Structures, Experimental and Predicted Distribution Coefficients (log$D$) of U(VI) Extracted by Phosphoryl-containing Podands
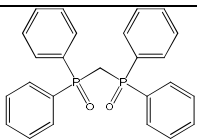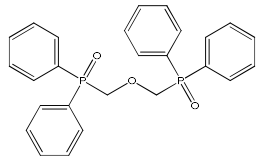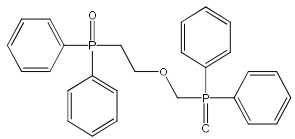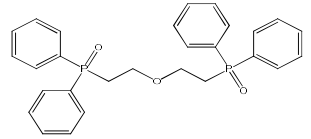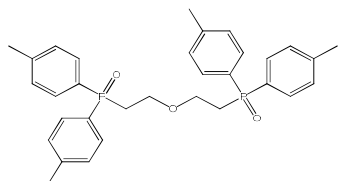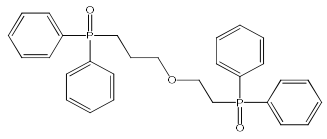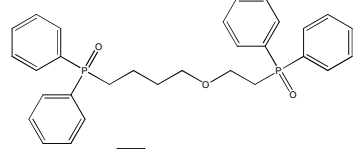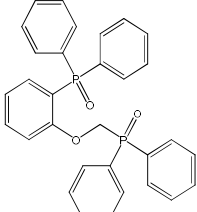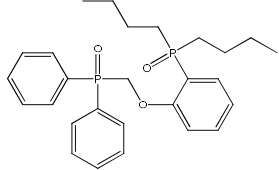
No.	Ligand structure	LogD (Experimental)	GRINd-3D-QSPR (Predicted)	2D-QSPR (Predicted)
1		2.58	2.66	2.58
2		0.1	0.26	0.38
3		0.51	0.69	0.52
4		0.75	0.59	0.64
5		1.05	1.06	1.24
6		0.85	0.73	0.31
7		0.45	0.32	0.15
8		0.84	0.98	0.71
9		0.95	1.12	0.68

Table 1. Continued
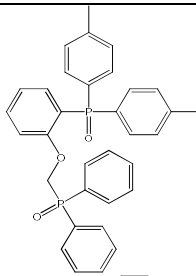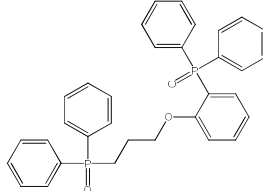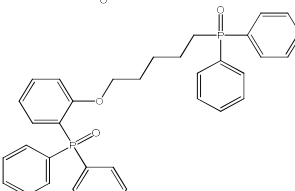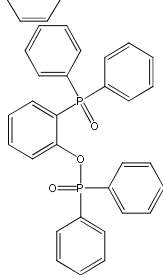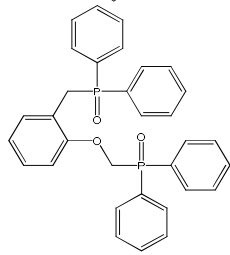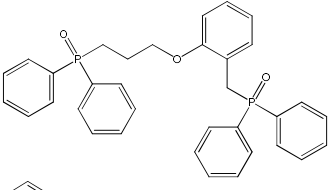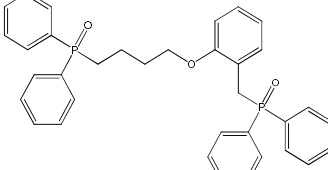
No.	Structure	Col1	Col2	Col3
10		1.20	0.9	0.88
11		0.33	0.37	0.47
12		0.42	0.52	0.14
13		0.47	0.41	0.23
14		0.67	0.76	0.78
15		0.02	0.13	0.22
16		0.26	0.36	0.31

Table 1. Continued
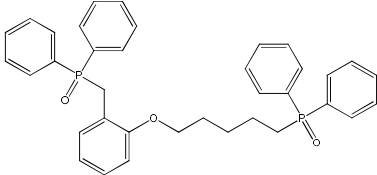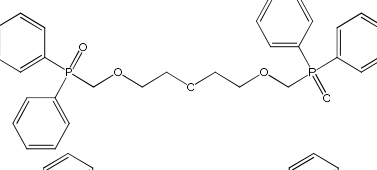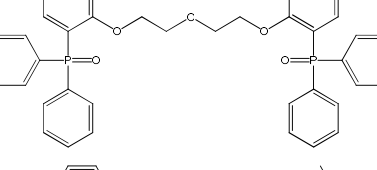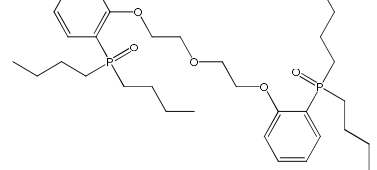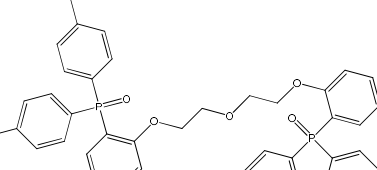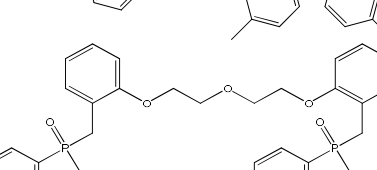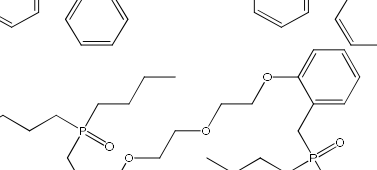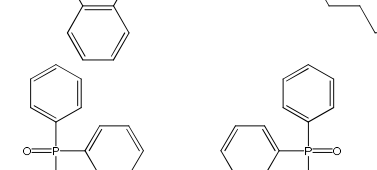
17		0.26	0.28	0.32
18		0.31	0.23	0.04
19		-0.87	-0.79	0.01
20		0.62	0.61	0.76
21		0.30	0.23	0.48
22		-0.20	-0.16	0.16
23		1.20	1.36	1.23
24		0.65	0.44	0.3

Table 1. Continued
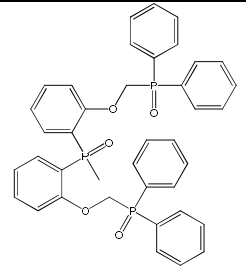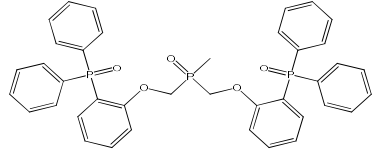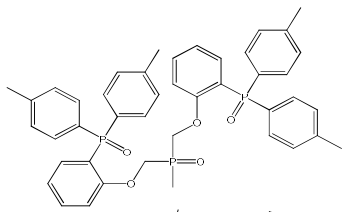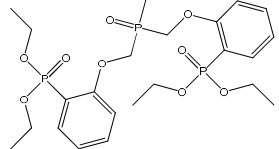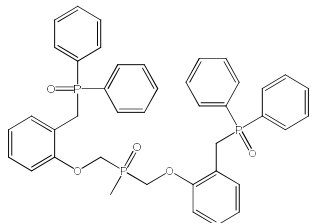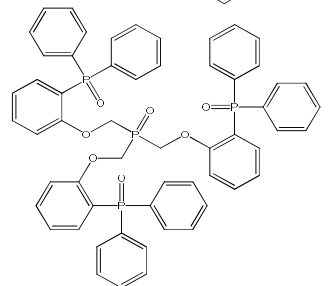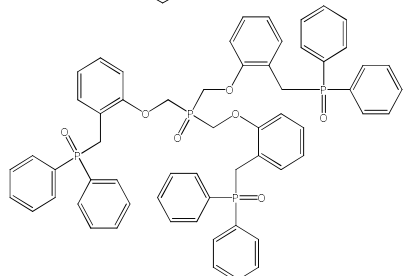
25		1.98	2.07	2.13
26		1.42	1.24	1.42
27		1.67	1.69	1.77
28		0.16	0.25	0.5
29		1.72	1.62	1.71
30		1.16	1.03	1.18
31		1.62	1.81	1.17

Table 1. Continued
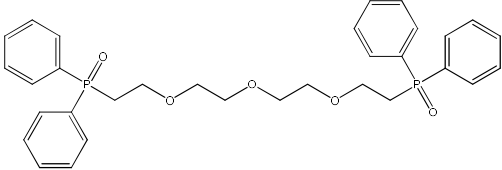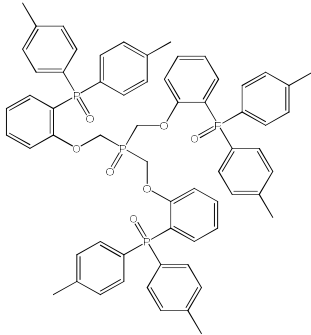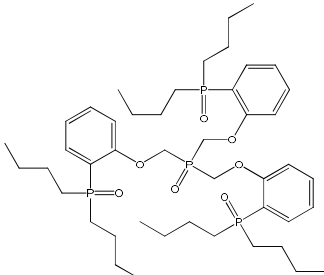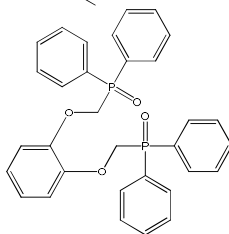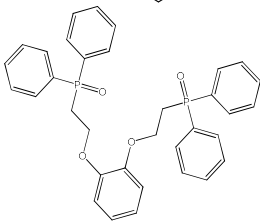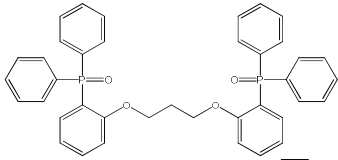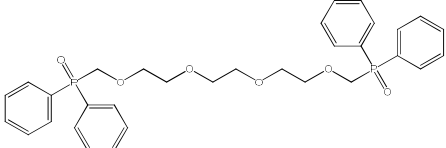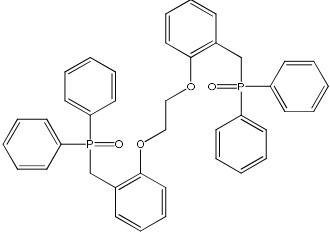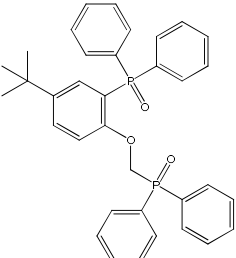
32		0.09	-0.08	-0.01
33		1.81 (0.05)	1.42	1.72
34		1.58 (0.05)	1.11	1.64
35		-0.27 (0.02)	0.15	0.43
36		0.39 (0.02)	0.48	0
37		-0.09 (0.01)	0.16	0.08
38		0.28 (0.02)	0.39	0.06

Table 1. Continued

39		-0.19 (0.01)	0.07	0.16
40		1.03 (0.05)	0.8	1.03

informative factors and generate a more predictive model. The FFD variable selection procedure was done as implemented in Pentacle software. Partial least square (PLS) regression analysis [35], and multi-linear regression (MLR) were used to predict the logD of U(VI) extracted by phosphoryl-containing podands. All calculations were performed in MATLAB (version 7.6.0., Math Works, Inc.).

RESULTS AND DISCUSSION

The distribution coefficient represents the extraction ability and is defined as the ratio of metal ion concentration in the organic phase (Co) to that in the aqueous phase (C) ($D = C_o/C$). As could be seen from Table 1, the structures of the ligands containing phosphine oxide groups with polyether linkers between P=O groups form a 1:1 complex uranyl cation. As mentioned above, structural aspects of the extractants play a key role in the separation processes and extraction efficiency. Molecular topology, the length of the polyether linkers, and the substituents at the phosphorus atoms of phosphoryl-containing podands have a significant effect on the process of extraction and should be considered [36].

Combining chemoinformatics and 3D molecular modeling approaches might be very useful for the development of new metal binders [8]. It is widely believed that 3D descriptors should provide better descriptions of the binding interactions. However, most 3D methods suffer from two constraints. First, the correct conformation of a molecule must be used, which may not even be the lowest energy conformation, to compare structurally different compounds; second, the compounds must be properly aligned, a step that is time-consuming and may introduce user bias [37]. The Grid Independent (GRIND) descriptors [27] were developed to overcome the alignment problem. Considering the high ability of GRIND variables to explain the relationships and identify important mutual distances between the molecular features of a compound, it is used to investigate the main interactions involved complexing of uranyl cation phosphoryl-containing podand ligands.

The GRIND descriptors were related to log values using partial least squares (PLS) analysis. The optimum number of PLS components (latent variables, LV) was chosen by monitoring changes in the model´s predicting index evaluated by applying the leave-one-out (LOO) cross-validation (q^2) procedure. Validation of the model was performed internally and externally using a cross-validation method and test set respectively. In the final model, a total of 75 descriptors were derived after variable selection FFD. The PLS analysis resulted in a model with three latent variables and a correlation coefficient of calibration (R^2_{cal}) of 0.932 with a standard error of calculation (SEC) of 0.188. We tested the predictivity of the obtained models with a test set of eight phosphoryl ligands proposed by Varnek *et al.* [23] for

structure see Table 1 (compounds no. 33-40). The cross-validation of the model by the LOO technique yielded q^2 values of 0.794 and by external validation of the model, the correlation coefficient of prediction (R^2_{Pred}) value of 0.542 with a standard error of prediction (SEP) of 0.539 was obtained. Figure 1 displayed the scatter plot of measured versus calculated logD of U(VI) extracted by phosphoryl-containing podand obtained by 2D-QSPR and GRIND-3D-QSPR models.

Figure 2 shows the PLS coefficient plot indicating the most important pairs of nodes that contribute negatively or positively to the logD values of U(VI) extracted by phosphoryl-containing podands. The five most significant GRIND descriptors with the highest impact on logD with their coefficient in the PLS model are indicated in Fig. 2. To gain a deeper insight into the model, the variables with the highest impact on logD values were inspected in more detail. The largest peak related to cross-correlogram DRY-TIP. Variable 421, DRY-TIP: distance 2.8-3.2 Å, explained the largest impact

on logD with an inverse relationship. As mentioned above, the DRY probe represents hydrophobic interactions and the TIP probe displays the shape and size of the ligands.

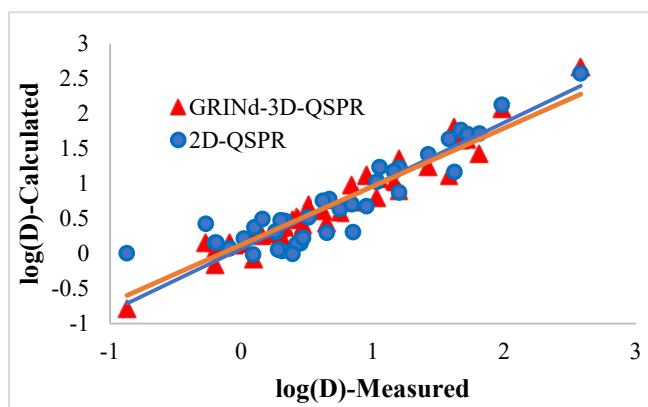**Fig. 1.** Scatter plot of measured versus calculated distribution coefficients (logD) of U(VI) extracted by phosphoryl-containing podands obtained by 2D-QSPR and GRIND-3D-QSPR models.
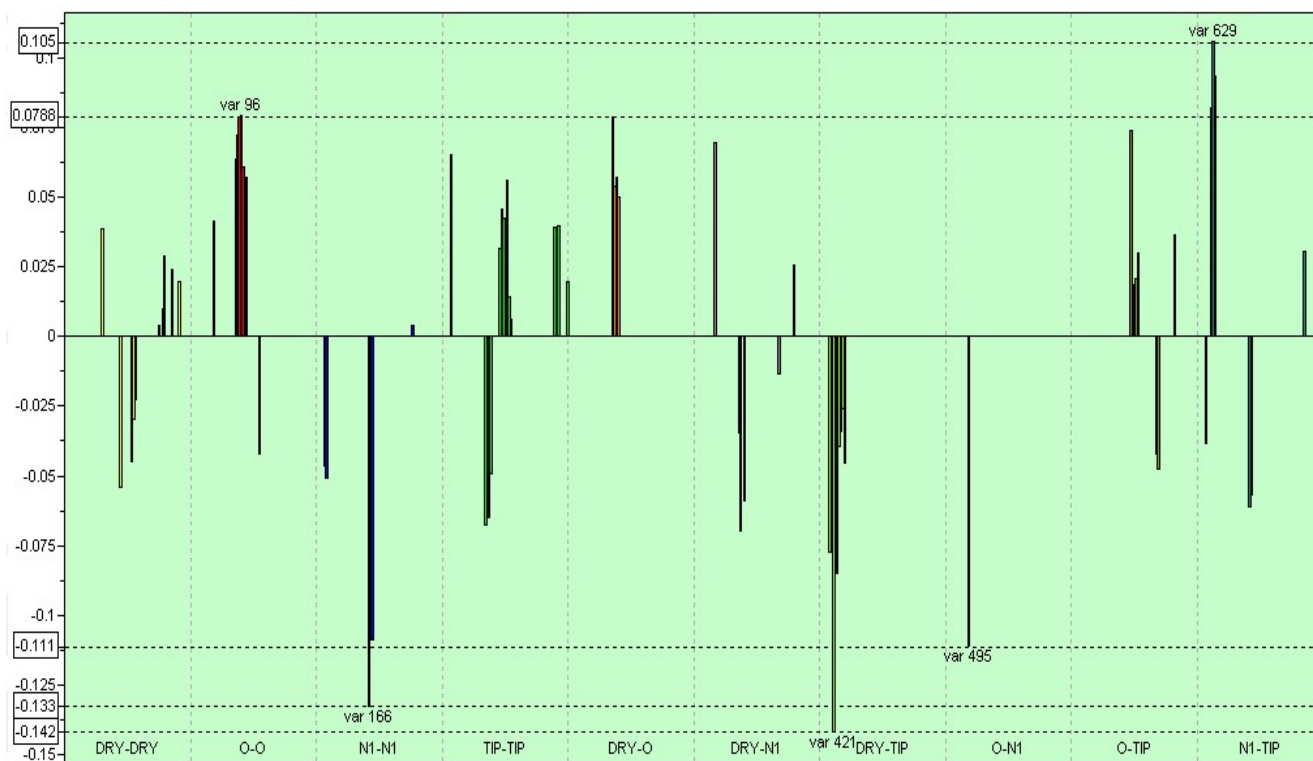

Fig. 2. The PLS coefficient plot of the GRIND variables used in the model. Different correlograms are separated by dotted lines and the pair probes are defined at the bottom. The most relevant variables are indicated by the variable number.

This indicated that adjacent a π system (aromatic backbone) and a bulky group in a distance of about 3 Å can reduce the interaction between the ligand molecules and metal ions. Phosphoryl legends like M22 and M28 with alkyl chains showed the highest value of variable 421 while molecules like M01 and M25 with the high logD values had the lowest value of this variable. It is well known that the DRY probe favorably interacts with different types of π systems (aromatic or vinyl type), but does not have a high affinity to aliphatic moieties. The next two effective peaks related to hydrogen bond acceptor-donor interactions, including variable 166, N_1-N_1: distance 11.2-11.6 Å with an inverse effect on logD and variable 96, O-O: distance 10.8-11.2 Å with a positive impact on logD values. The N1 probe represents the interaction with hydrogen bond (HB) donor groups whereas the O probe represents the interaction with hydrogen bond acceptor groups. Hydrogen bonding may be considered a hard acid-base interaction and strong hydrogen bonding usually requires a hard proton donor and acceptor [38]. Molecules with phenyl, as an electron-withdrawing group, directly connected to P=O make harder ligands than those ligands in which the phenoxy group was directlyconnected to the P=O group. Based on the hard-soft-acid-base (HSAB) principle [39], hard acids like UO_2^{2+} prefer to coordinate the hard bases hence the molecules like M01 and M05 with withdrawing phenyl groups are harder bases than M28 and M19 with phenoxy groups, have stronger affinity towards hard metal ions and show higher logD values. Figure 3 shows a graphical display of this variable for the ligands with the highest logD (M01), and the lowest logD (M19) ligands. In contrast, the O probe representing the hydrogen bond acceptor showed a positive impact on logD values. Molecules of M04 and M03 with polyether spacer are softer bases than M30 and M26 and show less tendency to the hard metal ion and had low logD values. Figure 4 shows a graphical display of variable 96 for the ligands with the highest logD (M01), and the lowest logD (M19) ligands. The two next significant variables are related to the N1 probe namely: variable 629, N1-TIP: distance 3.2-3.6 Å and variable 495, O-N1: distance 4.8-5.2 Å with positive and negative impact on logD values respectively. The importance of the N1-TIP variable indicates the favorable position of a hydrogen bond donor site or a polar group with respect to the size and shape of a phosphoryl ligand is significant in interactions with uranyl metal ions. Variable 495, O-N1: distance 4.8-5.2 Å indicated that adjacent of the donor and acceptor groups in the distance of about 5 Å can reduce the interaction between the ligand molecules and uranyl metal ions and decrease the logD values.

We also developed some simple, valid, and predictive QSPR models, able to correlate and predict logD values of U(VI) extracted by phosphoryl-containing podands.
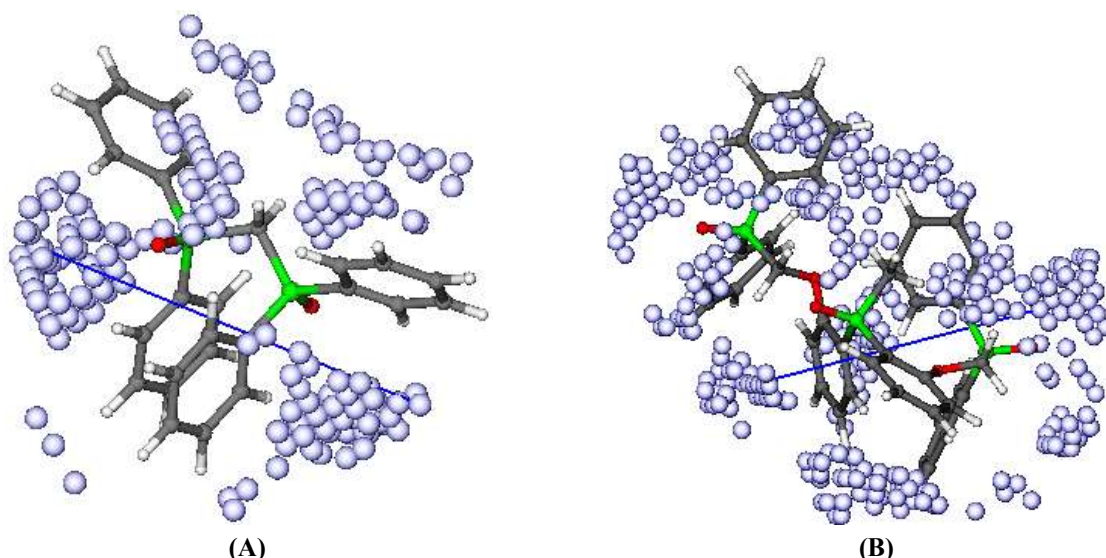

(A)   **(B)**

Fig. 3. Graphical display of GRIND variable 166, N_1-N_1: distance 11.2-11.6 Å for A: the most efficient (M01) and B: the least efficient (M019) phosphoryl-podand ligands.

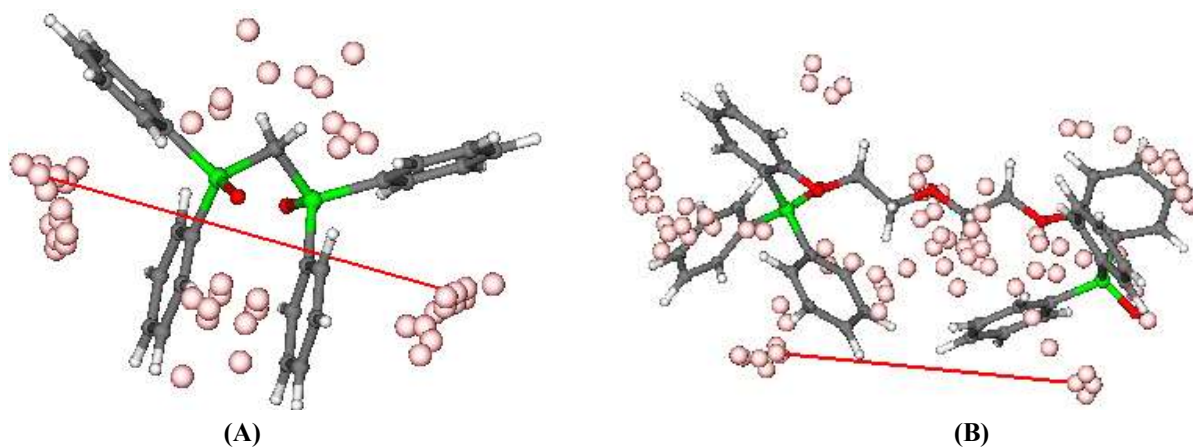| (A) | (B) |

Fig. 4. Graphical display of GRIND variable 96, O-O: distance 10.8-11.2 Å for A: the most efficient (M01) and B: the least efficient (M019) phosphoryl-podand ligands.

Table 2. The Performance of 2D-QSPR Statistical Parameters

	SEC	SEP	R^2_{cal}	R^2_{pred}	Q^2	R^2_{adj}	Equation
1	0.556	0.544	0.352	0.670	0.277	0.330	logD = -0.364-0.762 Mor17m
2	0.385	0.531	0.689	0.771	0.563	0.667	logD = 54.766-12.326 BEHm2+2.78 GGI9
3	0.285	0.552	0.829	0.624	0.768	0.811	logD = -76.71+18.15BEHm1 -3.967GATS3m+1.924GATS4m
4	0.277	0.397	0.840	0.769	0.778	0.816	logD = -68.522+17.553 BEHm1-2.189 GATS3m -2.1099 GATS2m-34.514 Qmean
5	0.244	0.357	0.875	0.805	0.799	0.852	logD = -65+1.882GGI9-2.292 GATS2m -1.253 MAXDN+15.393 BEHm1-9.3 qn_{max}
6	0.265	0.358	0.823	0.754	0.732	0.796	PLS model with 4 latent variables

Statistical characteristics of the best MLR models selected by the ERM feature selection along with the equations of QSPR models shown in Table 2. The predicted values of the logD values calculated from the five-variable MLR model are presented in Table 1.

Referring to the rule of thumb of *"five or six data points per descriptor"* [40], we calculated different models by increasing the number of involved descriptors up to five descriptors. The first significant descriptor selected by ERM was Mor17m (3D-MoRSE-signal 17/weighted by atomic masses) with a negative impact and high correlation ($r \approx 0.6$) of this variable with logD. The appearance of a 3D-MoRSE descriptor that encodes the 3D structure of a molecule reveals the role of steric interactions of phosphoryl ligands in complexing with uranyl ions and logD. Two topochemical Burden eigenvalues descriptors [41] including BEHm1 and BEHm2 (highest eigenvalue no.1 and 2 of Burden matrix/weighted by atomic masses respectively) and three 2D autocorrelations namely GATS2m, GATS3m, and GATS4m (Geary autocorrelation-lag 2, 3 and 4/weighted by atomic masses respectively), which explain the topological structure of a molecule were involved in the QSPR models [42]. Maximal electrotopological negative variation (MAXDN) shows an inverse effect on logD. It represents the maximum negative intrinsic state difference in the molecule and can be related to the nucleophilicity of the molecule [43]. On the other hand, the MAXDN descriptor could simply be related to the electron-donating abilities of phosphoryl ligands in

complexing with U(VI). The topological charge index of order 9 (GGI9), mean absolute charge (Q_{mean}) and maximum negative charge (qn_{max}) explain the importance of electrostatics and charge transfer interactions in the distribution coefficient of U(VI) extracted by phosphoryl-containing podands.

The PLS analysis on 16 Dragon selected descriptors, resulted in a model with four latent variables and correlation coefficient of calibration (R^2_{cal}) of 0.791 with a standard error of calculation (SEC) of 0.220, and a cross-validated of $q^2 = 0.732$, and significance value (F) = 801.7

As mentioned above we checked the predictivity power of models obtained with a test set of eight phosphoryl ligands proposed by Varnek *et al.* [23]. The predictive ability of the GRIND was poor ($R^2_{Pred} = 0.542$), but the performance of most 2D-QSPR models (Table 2) in the prediction of the external test set was higher than GRIND 3D-QSPR.

The applicability domain (AD) is a theoretical region in the space defined by the variables of the model and the modeled response, for which a given QSPR should make reliable predictions [44]. The analysis of AD of the ERM-PLS model and the reliability of the predictions are verified by the leverage approach, which is based on computing the leverage, h*, for each compound for which the QSPR model is used to predict the property under study [45]. The warning leverage is generally fixed at 3k/n, k being the number of model parameters and n being the number of training set compounds. The analysis of the applicability domain of

GRIND and the five-variable QSPR model displayed in Fig. 5. Figure 4A reveals the presence of just one chemical outlier (M35) of the GRIND model. 2D-QSPR model showed two response outliers namely M35 of the external test set and M19 of the train set. Both models displayed no structure-influential compound for the training set and prediction set (Fig. 5B). The statistics of the models were not significantly affected when omitting these compounds.

We also internally validated the models obtained by the Y-randomization test. The randomization technique consists of giving random values to the dependent variable and constructing a model with the real input descriptors. This randomization is repeated several times, and the resulting data are trained against real independent variables [46]. The **y**-randomizations performed imply that acceptable models were obtained for the given data sets by the current modeling method and they did not show any chance correlation [47]. The average values of R^2 and Q^2 (50 times) resulting from the **y**-randomization test for the GRIND model were 0.321 ± 0.094 and 0.052 ± 0.038 respectively. For the five-variable QSPR model, the R^2 of 0.287 ± 0.124 and Q^2 of 0.078 ± 0.054 from the **y**-randomization test were achieved.

Table 3 shows the statistical results of r_m^2 metrics, Golbraikh, and Tropsha criteria for validation tests of two 2D-QSPR and 3D-QSPR models. Predictive and reliable models are those with average r_m^2 values above the cutoff of 0.5 and with an Δr_m^2 value lower than 0.2 [48].
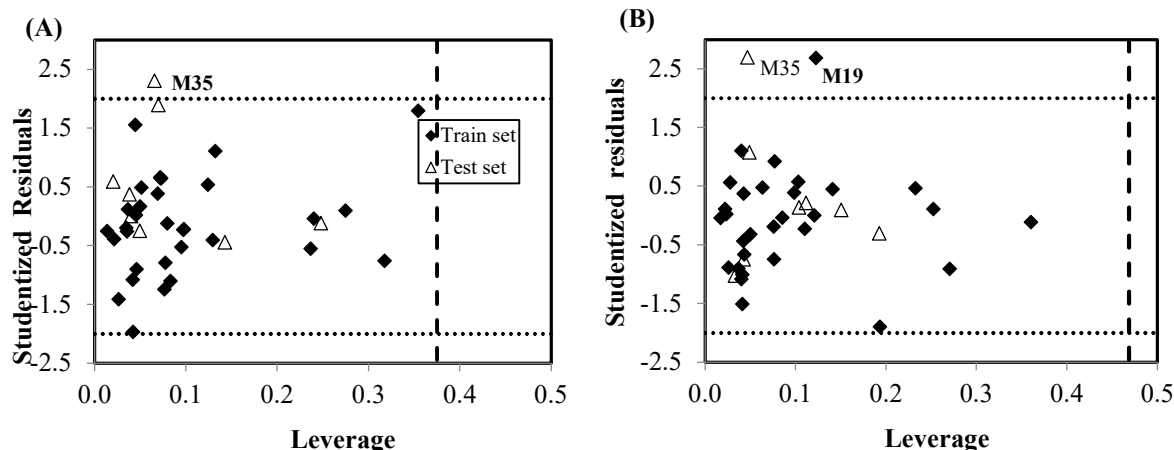

Fig. 5. Plot of standardized residuals *versus* leverages for A: GRIND B: 2D-QSPR models. The dotted lines represent ±2 studentized residual, dash line represents warning leverage.

Table 3. The Results of r_m^2 Metrics, Golbraikh, and Tropsha Criteria for Validation Tests of two 2D-QSPR and 3D-QSPR Models

QSAR model	r_m^2	r_{0m}^2	Δr^2_m	r^2	$\left\|r_0^2 - r'^2_0\right\|$
2D-QSPR	0. 839	0.833	0.007	0.808	0.019×10^{-2}
3D-QSPR	0.915	0.908	0.011	0.881	0.023×10^{-2}
Golbraikh and Tropsha criteria	-	>0.500	<0.200	>0.600	<0.300

For regressions through the origin, *i.e.* predicted *versus* observed activities, or observed versus predicted activities, at least one, but preferably both of the correlation coefficients for r_0^2 or $r_0'^2$ should be near r^2 [49,50]. Taking Table 3 into consideration, all statistical findings from our models met Golbraikh and Tropsha criteria, demonstrating the models' good predictive capacity.

CONCLUSIONS

From the GRIND variables involved in the PLS model the identification of some key molecular features and their position in the extractants' structure, which is crucial in the complexation and extraction process, would be possible. We also developed some simple, valid, and predictive 2D-QSPR models, able to correlate and predict the distribution coefficient of phosphoryl-podands in the extraction of uranyl cation aqueous solution in 1,2-dichloroethane. The performance of 2D-QSPR in the prediction of the external test set was higher than GRIND 3D-QSPR.

Considering the variables involves in models obtained, it's concluded that steric hindrance, electrostatic forces, charge transfer interactions, and electron-donating abilities of extractant molecules had important impacts on the distribution coefficient of U(VI) extracted by phosphoryl ligands. The obtained results could be led to the design and development of new highly efficient extracts which allow cost savings by reducing the laboratory resources needed and the time required to investigate and design new compounds by desired properties.

REFERENCES

[1] V.S. Kislik, Solvent Extraction: Classical and Novel Approaches. Elsevier, 2012.

[2] C. Hill, Overview of Recent Advances in An(III)/Ln(III) Separation by Solvent Extraction. In: Ion Exchange and Solvent Extraction. Ion Exchange and Solvent Extraction Series. CRC Press (2009) 119.

[3] Z. Kolarik, Chem. Rev. 39 (2008) 4208.

[4] B.P. Hay, T.K. Firman, G.J. Lumetta, B.M. Rapko, P.A. Garza, S.I. Sinkov, J.E. Hutchison, B.W. Parks, R.D. Gilbertson, T.J.R. Weakley, J. Alloys. Compd. 374 (2004) 416.

[5] J.D. Walker, M.C. Newman, M. Enache, Fundamental QSARs for Metal Ions. Taylor & Francis, New York, 2012.

[6] P. Comba, Coord. Chem. Rev. 185-186 (1999) 81.

[7] S.M. Ali, D.K. Maity, S. De, M.R.K. Shenoi, Desalination 232 (2008) 181.

[8] A. Varnek, V. Solov, Quantitative Structure-Property Relationships in Solvent Extraction and Complexation of Metals. In: B.A. Moyer (Ed.), Ion Exchange and Solvent Extraction. Ion Exchange and Solvent Extraction Series. CRC Press (2009) 319.

[9] A. Varnek, G. Wipff, Solvent. Extr. Ion Exc. 17 (1999) 1493.

[10] A. Boda, S.M. Ali, K.T. Shenoy, S.K. Ghosh, Sep. Sci. Tech. 48 (2013) 2397.

[11] T. Attapong, K. Hong-Ming, M. Nakarin, L. Narin, L. Alisa, W. Jirut, Int. J. Quantum. Chem. 71 (2012) 1634.

[12] I. Massova, P.A. Kollman, Perspect. Drug Discov. Des. 18 (2000) 113.

[13] X. Ye, S. Cui, V.F. de Almeida, B. Khomami, J. Phys. Chem. B 117 (2013) 14835.

[14] N. Sieffert, G. Wipff, J. Phys. Chem. A 110 (2006) 1106.

[15] K. Yoshizuka, Anal. Sci. 20 (2004) 761.

[16] F. Shiri, M. Salahinejad, N. Momeni-Mooguei, M.J.J.o.R. Sanchooli, J. Recept. Signal Transduct.

41 (2021) 59.

[17] A. Hajihosseinloo, M. Salahinejad, M.K. Rofouei, J.B. Ghasemi, Main Group Chem. 21 (2022) 431.

[18] H. González-Díaz, F.J. Prado-Prado, J. Comput. Chem. 29 (2008) 656.

[19] M. Grover, B. Singh, M. Bakshi, S. Singh, Pharm. Sci. Technol. Today 3 (2000) 28.

[20] A. Varnek, D. Fourches, N. Kireeva, O. Klimchuk, G. Marcou, A. Tsivadze, V. Solov'ev, Radiochimica Acta 96 (2008) 505.

[21] A. Varnek, D. Fourches, N. Sieffert, V.P. Solov'ev, C. Hill, M. Lecomte, Solvent Extr. Ion Exc. 25 (2007) 1.

[22] A. Varnek, D. Fourches, V. Solov'ev, O. Klimchuk, A. Ouadi, I. Billard, Solvent Extr. Ion Exc. 25 (2007) 433.

[23] A. Varnek, D. Fourches, V.P. Solov'ev, V.E. Baulin, A.N. Turanov, V.K. Karandashev, D. Fara, A.R. Katritzky, J. Chem. Inf. Model 44 (2004) 1365.

[24] A. Chagnes, A. Moncomble, G. Cote, Solvent Extr. Ion Exc. 31 (2013) 499.

[25] G. Cruciani, E. Carosati, S. Clementi, Three-Dimensional Quantitative Structure-Property Relationships. In: Camille GW (ed) The Practice of Medicinal Chemistry (Second Edition). Academic Press, London, 2003, 405.

[26] T. Langer, S.D. Bryant, 3D Quantitative Structure-Property Relationships. In: W. Camille Georges (Ed.), The Practice of Medicinal Chemistry (Third Edition). Academic Press, New York, 2008, p. 587.

[27] M. Pastor, G. Cruciani, I. McLay, S. Pickett, S. Clementi, J. Med. Chem. 43 (2000) 3233.

[28] J. Ghasemi, M. Rofouei, M. Salahinejad, J. InclPhenom. Macro. Chem. 70 (2011) 37.

[29] M. Salahinejad, E. Zolfonoun, Solvent Extr. Ion Exc. 32 (2014) 59.

[30] A.N. Turanov, V.K. Karandashev, V.E. Baulin, Radiokhimiya 40 (1998) 36.

[31] A. Duran, G.C. Martinez, M. Pastor, J. Chem. Inf. Model 48 (2008) 1813.

[32] A.G. Mercader, P.R. Duchowicz, F.M. Fernández, E.A. Castro, J. Chem. Inf. Model 50 (2010) 1542.

[33] A.G. Mercader, P.R. Duchowicz, F.M. Fernández, E.A. Castro, J. Chem. Inf. Model 51 (2011) 1575.

[34] M. Baroni, G. Costantino, G. Cruciani, D. Riganelli, R. Valigi, S. Clementi, Quant. Struct-Act Rel. 12 (1993) 9.

[35] S. Wold, M. Sjostrom, L. Eriksson, Chemom. Intell. Lab. Syst. 58 (2001) 109.

[36] A.N. Turanov, V.K. Karandashev, V.E. Baulin, Solvent Extr. Ion Exc. 17 (1999) 525.

[37] P. Cratteri, M.N. Romanelli, G. Cruciani, C. Bonaccini, F. Melani, J. Comput.-Aided Mol. Des. 18 (2004) 361.

[38] S. Ahuja, Chromatography and Separation Science, Separation science and technology. Academic Press, 2003.

[39] R.G. Pearson, J. Am. Chem. Soc. 85 (1963) 3533.

[40] J.G. Topliss, R.P. Edwards, J. Med. Chem. 22 (1979) 1238.

[41] F.R. Burden, Quant. Struct-Act. Rel. 16 (1997) 309.

[42] R. Todeschini, V. Consonni, Handbook of molecular descriptors. Wiley. com, 2008.

[43] L.B. Kier, L.H. Hall, Pharm. Res. 7 (1990) 801.

[44] P. Gramatica, QSAR. Combi. Sci. 26 (2007) 694.

[45] S. Dimitrov, G. Dimitrova, T. Pavlov, N. Dimitrova, G. Patlewicz, J. Niemela, O. Mekenyan, J. Chem. Inf. Comput. Sci. 45 (2005) 839.

[46] H. Van der Voet, Chemom. Intell. Lab. Syst. 25 (1994) 313.

[47] R.D. Clark, J. Comput. Aided Mol. Des. 17 (2003) 265.

[48] A. Golbraikh, A. Tropsha, J. Mol. Graph. 20 (2002) 269.

[49] K. Roy, P. Chakraborty, I. Mitra, P.K. Ojha, S. Kar, R.N. Das, J. Comput. Chem. 34 (2013) 1071.

[50] A. Tropsha, A. Golbraikh, Curr. Pharm. Des. 13 (2007) 3494.